Nonequilibrium Flow Analysis of a Two-dimensional MPD Arcjet

I.Funaki,* K.Toki,† and K.Kuriki††

Institute of Space and Astronautical Science, Kanagawa, Japan

Two-dimensional numerical analysis was conducted for a two-dimensional magnetoplasmadynamic (MPD) arcjet. Ionization and dissociation nonequilibrium was taken into account, and the plasma flow inside the discharge chamber was successfully analyzed. For both hydrogen and argon propellant, highly ionized and high temperature region near the cathode tip, so called cathode jet was simulated .

Nomenclature

a_m	=	magnetosonic velocity
B,B	=	self-induced magnetic field
B_0	=	inlet self-induced magnetic field
e	=	electricity
E	=	electric field
e_i	=	specific energy
Isp	=	specific impulse
j,j	=	current density
J	=	total discharge current
k	=	Boltzmann's constant
m	=	atomic or molecular mass
$\dot{m}$	=	mass flow rate
n_k	=	number density of species k
p	=	pressure
R	=	gas constant
t	=	time
T	=	temperature
u,u	=	velocity
u_0	=	inlet velocity
W	=	chamber width
x	=	coordinate
y	=	coordinate
α	=	ionization fraction
β	=	dissociation fraction
ε_0	=	permittivity in vacuum
ΔH	=	heat of formation
ε_D	=	dissociation energy per particle
ε_i	=	ionization energy per particle
γ	=	specific heat
μ_0	=	permeability in vacuum
ρ	=	total mass density
ρ_k	=	mass density of kth species
σ	=	electrical conductivity

Introduction

This paper describes the model and numerical simulations of the plasma flowfield of a magnetoplasmadynamic (MPD) arcjet. Even if we neglect the effect near the wall or so-called electrical sheath effect, the flowfield inside the discharge chamber of an MPD arcjet still comprises of many complicated physical phenomena such as discharge field, ionization, plasma acceleration, diffusive effect, etc. It is very difficult to treat all these phenomena owing to the limitation of the computation time as well as the stiffness of the analytical model. To establish a useful numerical tool for designing an MPD arcjet, one has to select some of important features of the flow from among all possible phenomena in the discharge chamber, and incorporate them to the model, and then check its consistency with the experimental data. To provide such experimental data, a multichannel two-dimensional MPD arcjet (2D-MPD)

*Researcher, Space Propulsion Division. Member AIAA.
†Associate Professor, Space Propulsion Division. Member AIAA.
††Professor, Space Propulsion Division. Fellow AIAA.

has been tested in the past several years in the Institute of Space and Astronautical Science (ISAS): the experimental data include not only thrust characteristics, but also flowfield distributions such as current contours, plasma density, current contours, and electron temperature. Now we are incorporating most possible effect step by step, checking both numerical and experimental data in order to decide necessary minimum model of the MPD arcjet.

From our previous study, the most idealized MHD model, that is, full ionization Ar plasma flow, can estimate thrust characteristics fairly well, and succeeded in evaluating geometric dependence of thrust generation.[1] However, from comparison between the numerical result and the flowfield data obtained from optical measurement of the 2D-MPD, the full ionization approximation resulted in an overestimation of temperature. Furthermore, such a model fails to evaluate molecular propellants, which is considered to be more appropriate for a practical application of the MPD arcjet. From one dimensional models, real gas effect is important for modeling molecular species.[2,3] In this study, to accomplish a minimum model for molecular propellants, ionization and dissociation nonequilibrium was taken into account and simulated for a two-dimensional MPD arcjet. Both Ar and H_2 are specified as propellant gases.

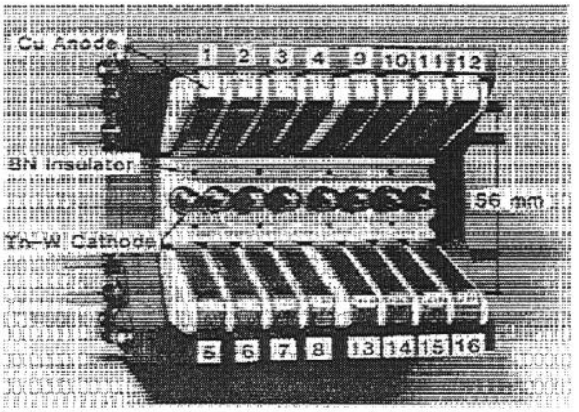

Fig.1 Two-dimensional MPD arcjet.

Numerical Model

Assumptions

Numerical analysis was conducted for a multicahnnel two-dimensional magneto-plasmadynamic arcjet (2D-MPD, Fig.1)[4]. The 2D-MPD approximates a two-dimensional plasma flow using eight discharge channels to secure the optical depth and to avoid non-uniform discharge along the line-of-sight. A lot of data of both the plasma flowfield inside the chamber as well as the thrust performance are available[5,6], and these experimental results can be compared with the numerical results. The following conditions were assumed to analyze the plasma flow of the 2D-MPD.

1) Plasma flow is strictly two-dimensional.
2) Steady-state flow is of interest, since the 2D-MPD is operated in quasi-steady mode.
3) Self-induced magnetic field is of interest. The Hall effect is neglected.
3) Argon and hydrogen is specified as propellant gas. Their dissociation and ionization processes follow chemically nonequilibrium kinetic model shown below. Quasi-neutrality applies.
4) Viscosity, thermal conductivity, electrical sheath, and radiation processes are neglected.
6) The plasma flow is accelerated from sub-magnetosonic speeds to super-magnetosonic speeds, where the magnetosonic speed is defined as:

$$a_m = \sqrt{\gamma RT + \frac{B_0^2}{2\rho\mu_0}} \qquad (1)$$

which is the propagating speed of small disturbances in the MHD flowfield.

Governing Equations

Time dependent equations are treated, in order to use a time-marching algorithm. In the MHD framework the displacement current in the Maxwell equations is neglected. The basic electromagnetic equations are:

Maxwell equations

$$\frac{\partial \mathbf{B}}{\partial t} = -rot\,\mathbf{E} \qquad (2)$$

$$\mathbf{j} = \frac{1}{\mu_0} rot\,\mathbf{B} \qquad (3)$$

Ohm's law

$$j = \sigma(\mathbf{E} + \mathbf{u} \times \mathbf{B}) \qquad (4)$$

Solving eq. (3) to (5) for the magnetic flux density

yields the induction equation,

$$\frac{\partial \mathbf{B}}{\partial t} = rot\left[\mathbf{u}\times\mathbf{B} - \frac{1}{\sigma\mu_e} rot\,\mathbf{B}\right]. \quad (5)$$

As for fluid equations, the Lorentz force term for the equation of motion and the Joule heating for the energy equation are taken into account. The inviscid Euler equations with electromagnetic source terms become:

overall mass conservation

$$\frac{\partial \rho}{\partial t} + \nabla(\rho\,\mathbf{u}) = 0 \quad (6)$$

equation of motion

$$\frac{\partial \rho\,\mathbf{u}}{\partial t} + \nabla(\rho\,\mathbf{uu} + p) = \mathbf{j}\times\mathbf{B} \quad (7)$$

energy conservation

$$\frac{\partial e_t}{\partial t} + \nabla\cdot\left[(e_t + p)\mathbf{u}\right] = \mathbf{j}\cdot\mathbf{E} \quad (8)$$

equation of state

$$p = \sum_i n_i\, k\, T \quad (9)$$

The mass density is related to the number densities through the following algebraic relation,

$$\rho = \sum_i m_i n_i\,. \quad (10)$$

Also, each species follows nonequlibrium rate equations of ionization and dissociation:

$$\frac{\partial \rho_i}{\partial t} + \nabla(\rho_i\,\mathbf{u}) = \dot{\rho}_i\,. \quad (11)$$

For hydrogen, the mixture is assumed to consist of four species: molecular hydrogen , atomic hydrogen, ionized hydrogen, and electron. For argon, the propellant is composed of atomic Ar, ion, and electron. With the assumption of electrical neutrality, the electron and ion concentrations are equal and one species' equation can be eliminated.

All the simulations were executed for the 2D-MPD arcjet (Fig.1). Applying the MHD equations for the Cartesian coordinates, the governing equations for flow variables can be transformed into a vectorized form

$$\frac{\partial}{\partial t}\begin{bmatrix}\rho\\ \rho u\\ \rho v\\ e_t\\ \rho_1\\ \vdots\\ \rho_n\end{bmatrix} + \frac{\partial}{\partial x}\begin{bmatrix}\rho u\\ \rho u^2 + p\\ \rho uv\\ (e_t + p)u\\ \rho_1 u\\ \vdots\\ \rho_n u\end{bmatrix} + \frac{\partial}{\partial y}\begin{bmatrix}\rho v\\ \rho uv\\ \rho v^2 + p\\ (e_t + p)v\\ \rho_1 v\\ \vdots\\ \rho_n v\end{bmatrix} = \begin{bmatrix}0\\ j_y B\\ -j_x B\\ j_x E_x + j_y E_y\\ \dot{\rho}_1\\ \vdots\\ \dot{\rho}_n\end{bmatrix} \quad (12)$$

where

$$e_t = \frac{1}{2}\rho\left(u^2 + v^2\right) + \sum_{i=\text{atom, ion, electron}} \frac{3}{2}\rho_i R_i T + \sum_{i=\text{molecular}} \frac{6}{2}\rho_i R_i T + \Delta H \quad (13)$$

is total energy, in which the vibrational energy mode for molecular species is assumed to be half excited. For the magnetic flux density, a scalar equation is derived.

$$\frac{\partial B}{\partial t} + \frac{\partial uB}{\partial x} + \frac{\partial vB}{\partial y} - \frac{\partial}{\partial x}\left(\frac{1}{\sigma\mu_0}\frac{\partial B}{\partial x}\right) - \frac{\partial}{\partial y}\left(\frac{1}{\sigma\mu_0}\frac{\partial B}{\partial y}\right) = 0 \quad (14)$$

Equations (12) and (14) govern the plasma flow inside the chamber of the 2D-MPD.

The electrical conductivity is given as the geometrical average of both Chapman-Cowling's σ_n and Spitzer-Härm's σ_t.[7] It depends on both temperature and electron density.

$$\frac{1}{\sigma} = \frac{1}{\sigma_n} + \frac{1}{\sigma_t} \quad (15)$$

Reaction model

For Ar, ionization and recombination processes are modeled according to the following equation:[8]

$$Ar + e^- \Leftrightarrow Ar^+ + e^- + e^- \qquad (16)$$

while for hydrogen, four dissociative processes and one ionization process were selected:

$$H_2 + H_2 \Leftrightarrow H + H + H_2 \qquad (17)$$

$$H_2 + M \Leftrightarrow H + H + M \quad (M = H, H^+) \qquad (18)$$

$$H_2 + e^- \Leftrightarrow H + H + e^- \qquad (19)$$

$$H + e^- \Leftrightarrow H^+ + e^- + e^- \qquad (20)$$

Chemical rate coefficients were taken from the work of Shoji et al.[9]

Calculation Procedure

Numerical Grid

Figure 2 shows the calculation grids used for comparison with the experimental data. At the anode

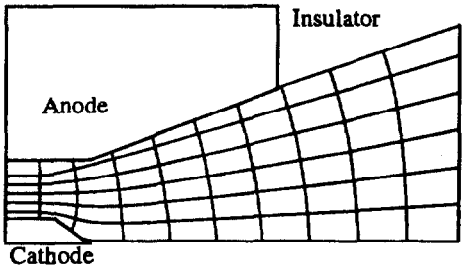

Flared anode, short cathode

Fig.2 Calculation grid.

end, the supersonic flow forms a jet separating from the anode boundary, where the inviscid model fails. To avoid this difficulty, the rapid expansion region at the anode end was replaced by an insulator under the assumption that the flow near the anode end will not affect the core flow between the electrodes.

Solver

Numerical analysis conducted here treat both plasma flowfield and electromagnetic field separately. Both the flow and the electromagnetic equations were discretized based on the finite difference method: for the Euler equation (12), the point implicit TVD-MacCormack scheme with Roe-Davis's dissipation term was extended to nonequilibrium flow;[10,11] for the induction equation (14), all derivatives were discretized using the central differencing method and solved by the SOR method, dropping the time dependent term because only the steady-state solution is of interest. Calculation time steps of both fields are proceeded independently and coupled together for every few hundred steps and convergence can be achieved.

Boundary Conditions

At the electrode surfaces, the tangential electric field component was fixed as zero, which forces the electrode surface to be an equipotential contour. At the inlet, the magnet flux density B_0 was given. In the case of the 2D-MPD, B_0 is related to the total discharge current J as

$$B_0 = \mu_0 J/2W, \qquad (21)$$

where W is the channel width of the 2D-MPD. At other boundaries, that is, outside the chamber, at the symmetry axis, and at the outlet boundary, the magnetic flux was set to zero. The electrodes and the insulator were treated as slip walls. As for the inlet and the outlet boundary conditions, subsonic inflow and supersonic outflow were specified. In this simulation, the inlet temperature was assumed to be 3,000 K.

Results and Discussion

In the following, numerical results for Ar and H_2 propellant are provided.

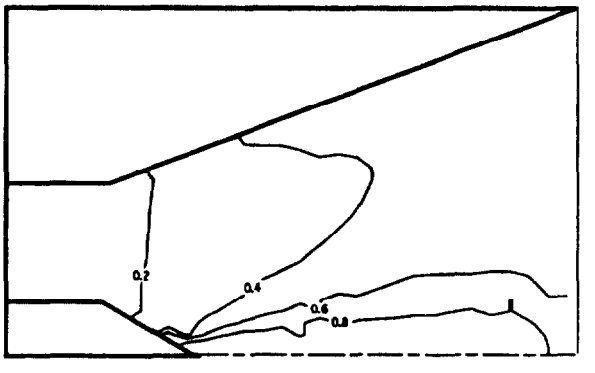

a) Ar

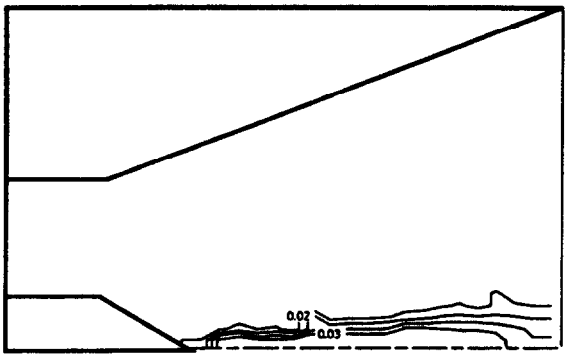

b) H_2

Fig.3 Ionization fraction (8kA, 2.5g/s).

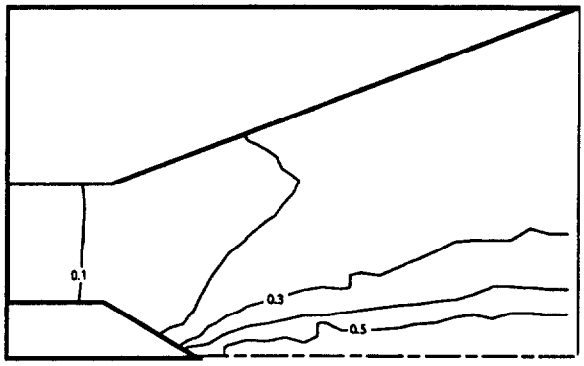

Fig.4 Dissociation fraction for H_2 (8kA, 2.5g/s).

At a condition J=8kA, $\dot{m}$=2.5g/s, targeted at medium Isp operation, ionization fraction in Fig.3 stays below one, which means disparity from full ionization. Not full ionization explains relatively low density field indicated in the experiment.[1] H_2's low ionization fraction is attributed to dissociative reaction as shown in Fig.4; heat energy is consumed in the dissociative process followed by ionization, which is localized to so-called cathode jet region. Once the ionization occurred in the cathode tip region, ionization fraction or dissociation fraction are frozen to certain values in the downstream part of the cathode jet. Such a frozen reaction will be typical nonequilibrium phenomenon that will occur in the MPD flow. Also, near the tip of the cathode, excessively high temperature was observed for both Ar and H_2 (Fig.5). Temperatures in the interelectrode region stays about 10,000 K for Ar and below 10,000 K for H_2, and the peak values at the cathode tip are 36,000 K and 18,000 K, respectively. Although these values are a bit higher than the experimental results, the simulations are considered to treat real gas effect for both propellants, that is, energy deposition into chemical processes.

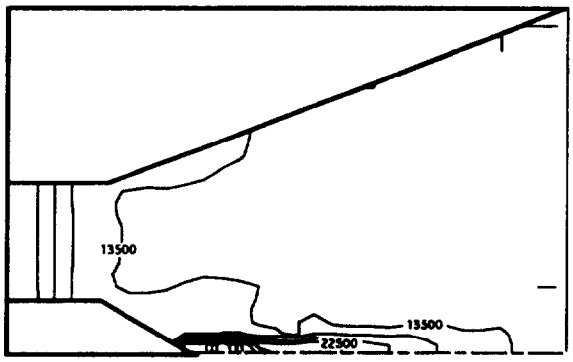

a) Ar

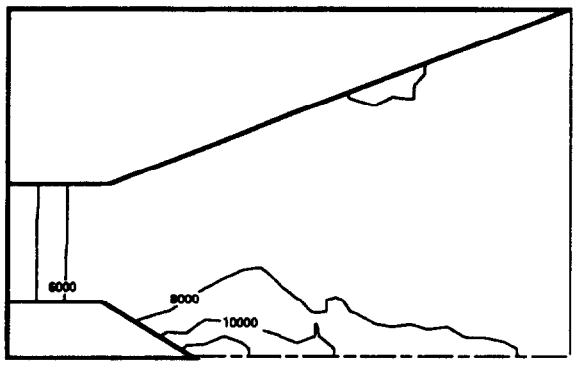

b) H_2

Fig.5 Temperature distribution (8kA, 2.5g/s).

Summary

Numerical simulation for the two-dimensional MPD arcjet (2D-MPD) was successfully conducted. To evaluate the plasma flow for both argon and hydrogen propellant, nonequilibrium ionization and dissociation processes were taken into account. Inclusion of these chemical processes made it possible to achieve realistic temperature distributions numerically, and the cathode jet, in which highly ionized plasma is confined near the cathode tip, was

simulated.

References

1 Funaki, I., Toki, K., and Kuriki, K., "Numerical Analysis of a Two-dimensional Magnetoplasmadynamic Arcjet ", to be appear to Journal of Propulsion and Power.

2 Sumida and Toki, K., "Real Gas Effect on the Magnetoplasmadynamic Arcjet", Journal of Propulsion and Power, Vol.7, No.6, 1991, pp.1072-1074.

3 Tahara, H., Mitsuo, K., Zhang, L., Kagaya, Y., and Yoshikawa, T., "Plasma Features in Quasisteady MPD Channels", 24th International Electric Propulsion Conf., IEPC-95-116, 1995.

4 Toki, K., Sumida, M., and Kuriki, K., "Multichannel Two-Dimensional Magnetoplasmadynamic Arcjet", Journal of Propulsion and Power, Vol.8, No.1, 1992, pp.93-97.

5 Nakayama, T., and Toki, K., and Kuriki, K., "Quantitative Imaging of the Magnetoplasmadynamic Flowfield", Journal of Propulsion and Power, Vol.8, No.6, 1992, pp.1217-1223.

6 Funaki, I., Toki, K., and Kuriki, K., "Effect of Electrode Configuration on the Performance of a Two-dimensional Magnetoplasmadynamic Arcjet", to be appear to Journal of Propulsion and Power.

7 Cambel, A.B., "Plasma Physics and Magnetofluidmechanics", McGRAW-HILL, 1963.

8 Subramaniam, V.V., and Lawless, J.L., "Onset in Magnetoplasmadynamic Thrusters with Finite-Rate Ionization", Journal of Propulsion and Power, Vol.4, No.6, 1988, pp.526-532.

9 Shoji, T., and Kimura, I., "Analytical Study on the Influence of Nonequilibrium Ionization for Current Flow Pattern and Flow Field of MPD Arcjets", AIAA paper 90-2609, 1990.

10 Yee, H.C., "A Class of High-Resolution explicit and implicit Shock-Capturing Method", NASA TM101088, 1989.

11 Liu, Y., and Vinokur, M., "Nonequilibrium Flow Computations. I. An Analysis of Numerical Formulations of Conservation Laws", Journal of Computational Physics, Vol.83, 1989, pp.373-397.